AGU PUBLICATIONS

Geophysical Research Letters

RESEARCH LETTER
10.1002/2017GL072770

Key Points:
- Unveiled earthquake interaction and verified earthquake triggering on Sagaing Fault, Myanmar
- Identified three positively stressed earthquake gaps on the Sagaing Fault with high seismic hazard
- The buildup of ΔCFS on two seismic gaps is equivalent to a tectonic loading over 10 years, even if conservatively estimated

Supporting Information:
- Supporting Information S1

Correspondence to:
X. Xiong,
xxiong@whigg.ac.cn

Citation:
Xiong, X., B. Shan, Y. M. Zhou, S. J. Wei, Y. D. Li, R. J. Wang, and Y. Zheng (2017), Coulomb stress transfer and accumulation on the Sagaing Fault, Myanmar, over the past 110 years and its implications for seismic hazard, *Geophys. Res. Lett.*, *44*, 4781–4789, doi:10.1002/2017GL072770.

Received 23 JAN 2017
Accepted 1 MAY 2017
Accepted article online 3 MAY 2017
Published online 21 MAY 2017

Coulomb stress transfer and accumulation on the Sagaing Fault, Myanmar, over the past 110 years and its implications for seismic hazard

X. Xiong[1,2], B. Shan[1], Y. M. Zhou[3], S. J. Wei[4,5], Y. D. Li[1], R. J. Wang[6], and Y. Zheng[1]

[1]Hubei Subsurface Multi-Scale Imaging Key Laboratory, Institute of Geophysics and Geomatics, China University of Geosciences, Wuhan, China, [2]Institute of Geodesy and Geophysics, Chinese Academy of Sciences, Wuhan, China, [3]Department of Earth and Atmospheric Sciences, Saint Louis University, St. Louis, Missouri, USA, [4]Earth Observatory of Singapore, Nanyang Technological University, Singapore, [5]Asian School of the Environment, Nanyang Technological University, Singapore, [6]GFZ German Research Centre for Geosciences, Potsdam, Germany

Abstract Myanmar is drawing rapidly increasing attention from the world for its seismic hazard. The Sagaing Fault (SF), an active right-lateral strike-slip fault passing through Myanmar, has been being the source of serious seismic damage of the country. Thus, awareness of seismic hazard assessment of this region is of pivotal significance by taking into account the interaction and migration of earthquakes with respect to time and space. We investigated a seismic series comprising10 earthquakes with $M > 6.5$ that occurred along the SF since 1906. The Coulomb failure stress modeling exhibits significant interactions among the earthquakes. After the 1906 earthquake, eight out of nine earthquakes occurred in the positively stress-enhanced zone of the preceding earthquakes, verifying that the hypothesis of earthquake triggering is applicable on the SF. Moreover, we identified three visible positively stressed earthquake gaps on the central and southern SF, on which seismic hazard is increased.

1. Introduction

The oblique convergence between the India and Sunda is accommodated by a partitioned system of some tectonic structures, the most significant of which is the Sagaing Fault (SF), a major N-S striking right-lateral strike-slip fault extending about 1200 km between 15°N and 27°N (Figure 1) [*Maung*, 1987; *Holt et al.*, 1991]. The SF, which links the Andaman Sea in the south and the Eastern Himalayan Syntaxis in the north, is considered to be one of the most active faults in the world with a present-day slip rate of about 2 cm/yr [*Maurin et al.*, 2010]. Geological studies indicate that the SF has accommodated about 330 km [*Curray*, 2005] to 450 km [*Mitchell*, 1993] of dextral displacement between its eastern and western sides since its formation during the Miocene [*Searle et al.*, 2007]. The accumulated strain is released in spasmodic slip events associated with earthquakes. As a result, the SF has experienced a long recorded history of seismic activity, including six $M \geq 7$ events since 1930 [*Hurukawa and Maung Maung*, 2011]. Since the SF cuts through the center of Myanmar and passes through some highly populated and rapidly developing cities, such as Nay Pyi Taw, Bago, Sagaing, Mandalay, and Yangon (Figure 1), a large population more than 17 million is exposed to a significant earthquake hazard. The great concern raises the question where the next large earthquake would most likely occur.

We address this question by investigating the evolution of the Coulomb stress and earthquake interaction on the SF in the last 110 years. Earthquake triggering due to change of Coulomb failure stress (ΔCFS) triggers an earthquake with positive ΔCFS, in contrast, negative ΔCFS delays the occurrence of subsequent events [*Stein*, 2003; *Freed*, 2005]. In recent 20 years, the earthquake triggering hypothesis has enjoyed the support from a number of studies on aftershock distribution [e.g., *King et al.*, 1994; *Toda et al.*, 1998], earthquake sequences [e.g., *Pollitz et al.*, 2003; *Shan et al.*, 2013], and triggering of moderate to large earthquakes [e.g., *Harris et al.*, 1995; *Deng and Sykes*, 1996] as well as earthquake hazard assessment [e.g., *Nalbant et al.*, 2005].

The purpose of this study is to investigate a seismic series comprising 10 earthquakes of $M > 6.5$ on the SF (Table 1 and Figure 1) since 1906. We calculated evolution of stress by merging key parameters such as coseismic slip, postseismic viscoelastic relaxation, and interseismic tectonic loading due to India-Sunda convergence. The correlation between the stress evolution and earthquake migration was checked by examining

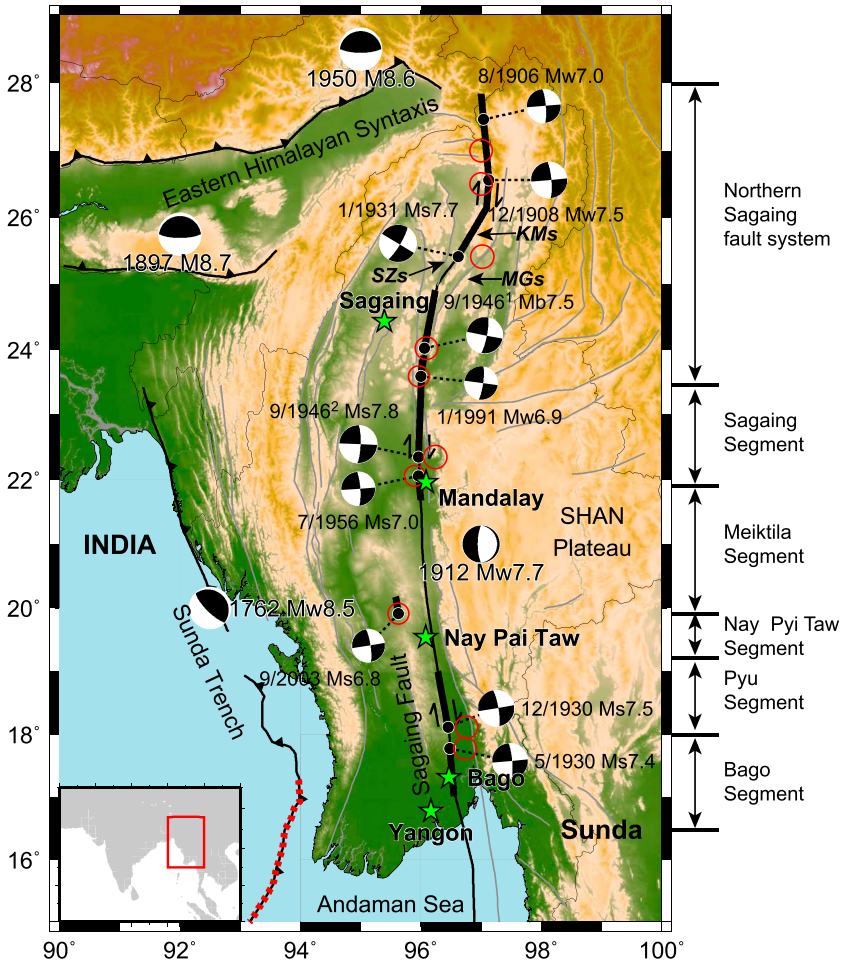

Figure 1. Map shows location of the SF region and 10 earthquakes ($M > 6.5$) along the fault from 1906 to 2003. The open red circles and beach balls display the proposed [*Maurin et al.*, 2010; *Kundu and Gahalaut*, 2012; *Hurukawa and Maung Maung*, 2011] and the modified epicenters in this study, respectively. The black beach balls indicate the large historical earthquakes. The black solid lines and black thick lines represent faults and ruptured segments, respectively. The grey lines are other active faults in this region. The red dashed line indicates the unruptured section on Sunda Trench. The green stars denote the cities with population more than 1 million. Shaduzup (SZs), Kamaing (KMs), and Mogang (MGs) segments are three strands on the northern Sagaing fault system [*Wang*, 2013]. Nay Pai Taw is the new capital of Myanmar, and Yangon is the largest and highest populated city of Myanmar. Inset shows study area at regional scale. The segments are labeled right of the figure, after *Wang* [2013].

the evolution of the ΔCFS on the rupture surfaces immediately before the earthquakes. We extended the calculation to the present to estimate current state of stress on various segments of the SF and identified the portion (s) possessing viable stress to trigger an earthquake. The inferred information is then used for the seismic hazard assessment in this region.

2. Earthquake Sequence and Source Parameters

In the past 110 years, many earthquakes occurred on/near the SF. *Hurukawa and Maung Maung* [2011] compiled a catalog consisting of 19 events of $M > 6$ during the period between 1930 and 2003. The earthquake-induced (static and postseismic) stress transfer of events with $M \leq 6.5$ affects ΔCFS only at local scale, and the rupture parameters determined by paleo-seismic studies have large uncertainties. Therefore, in this study, we focused on the earthquakes with $M > 6.5$. Hence, we compiled an earthquake sequence consisting of 10 events (Figure 1 and Table 1) by picking 8 from *Hurukawa and Maung Maung* [2011] and 2 from *Maurin et al.* [2010] and *Kundu and Gahalaut* [2012]. The locations of 9 out of 10 earthquakes are evidenced by ruptures on

Table 1. Historical Earthquakes Along With Associated Source Parameters Used in the Study and Accumulated ΔCFS Along the SF[a]

			Modified Epicenters				$\Delta\sigma_c$ (MPa)			$\Delta\sigma_c + p$ (MPa)			P(%)
No.	DD-MM-YYYY	Magnitude	Latitude	Longitude	Strike/Dip/Rake	Length/Width/Slip (km/km/ m)	$\Delta\sigma_{max}$	$\Delta\sigma_{ave}$	P(%)	$\Delta\sigma_{max}$	$\Delta\sigma_{ave}$	$\mu' = 0.2/0.4/0.6$
1	31-08-1906	M_w7.0	27.46	97.04	355°/80°/180°	42.7/13.5/0.96	–	–	–	–	–	–/–/–
2	12-12-1908	M_w7.5	26.56	97.13	355°/80°/180°	100.0/18.4/2.69	0.256	0.025	42	0.258	0.025	43/43/43
3	05-05-1930	M_s7.4	17.78	96.48	355°/80°/180°	84.3/17.3/2.19	1.2×10^{-5}	1.1×10^{-5}	0	1.2×10^{-5}	1.1×10^{-5}	0/0/0
4	03-12-1930	M_s7.5	18.12	96.45	350°/80°/180°	100.0/18.4/2.69	0.066	0.018	57	0.066	0.018	55/56/57
5	27-01-1931	M_s7.7	25.41	96.62	31°/80°/180°	140.6/20.8/4.07	0.032	1.8×10^{-3}	12	0.044	1.8×10^{-3}	21/17/14
6	12-09-1946	M_b7.5	24.02	96.06	11°/80°/180°	100.0/18.4/2.69	0.049	0.020	73	0.060	0.025	87/91/94
7	12-09-1946	M_s7.8	22.35	95.96	2°/80°/180°	166.7/22.2/5.01	0.241	0.034	54	0.259	0.036	60/58/56
8	16-07-1956	M_s7.0	22.06	95.96	356°/80°/180°	42.7/13.5/0.96	0.275	0.131	100	0.301	0.147	100/100/100
9	05-01-1991	M_w6.9	23.59	96.00	8°/80°/180°	36.0/12.7/0.78	9.932	−3.801	21	10.22	−3.502	20/20/22
10	21-09-2003	M_s6.8	19.91	95.63	351°/80°/180°	30.3/11.9/0.63	0.002	0.001	0	0.008	0.008	0/0/0

[a]The 1906 and 1908 events are taken from *Maurin et al.* [2010] and *Kundu and Gahalaut* [2012], and the others are from *Hurukawa and Maung Maung* [2011]. μ', effective coefficient of friction; $\Delta\sigma_c$, coseismicΔCFS; $\Delta\sigma_c + p$, coseismic + postseismicΔCFS; $\Delta\sigma_{max}$, $\Delta\sigma_{ave}$, maximum and averaged ΔCFS on the rupture. *P*(%) indicates the percentage of the rupture length with $\Delta\sigma \geq 0.01$ MPa.

surface confirmed by field work [*Wang*, 2013], except the 1931 earthquake, the locations of hypocenter and rupture of which is still enigmatic. In the study, we chose the Kamaing (KMs) as the rupture source, following Wang's suggestion [*Wang*, 2013]. However, since the possibility of a source on the Mogang (MGs) cannot be ruled out due to sparse seismic intensity records and unavailability of isoseismal map, we conducted comparison test by considering MGs as the source and presented the results in the supporting information.

In calculation, ΔCFS was obtained by projecting earthquake-induced two-order stress tensor on a special fault plane, which is known as receiver fault. The rake angles of rupture and receiver fault are set to be 180° following the geologic fault mapping [*Maung*, 1987]. We set the dip angles of rupture and receiver fault to be 80° as suggested by *Tsutsumi and Sato* [2009]. Since the locations of historical earthquakes are not well constrained and large earthquakes mainly occurred on active faults, we slightly modified the locations of epicenters of historical earthquakes to shift them on the SF.

Since the rupture properties of historical earthquakes are poorly constrained, the source parameters are derived from magnitude by using empirical scaling relationships. We calculated the length and width of rupture, average displacement by either M_s or M_w based on the empirical equation given by *Wells and Coppersmith* [1994], as the difference between the magnitude scale (M_s and M_w) is negligible for the earthquakes with $M > 5.7$ [*Wells and Coppersmith*, 1994]. The model parameters for the historical earthquakes are shown in Table 1. Here we assume uniform slip on the rectangle fault, as detail slip distributions for these earthquakes are not available. However, different empirical scaling relationships result in different source parameters. To verify the stability of results due to the uncertainties of source parameters, we conducted comparison experiment using the empirical scaling relationships proposed by *Kanamori and Anderson* [1975].

3. Models and Methods

3.1. ΔCFS Calculation

We calculated the ΔCFS by using the expression [*Scholz*, 1990]

$$\Delta\mathrm{CFS} = \Delta\tau - \mu' \Delta\sigma_N$$

where τ, σ_N, and μ' represent shear stress (in Pa), normal stress (in Pa), and effective coefficient of friction, respectively.

In the present study, the evolution of ΔCFS in the Myanmar region was computed by integration of coseismic static and postseismic viscoelastic relaxation stress transfer since the 1906 M_w7.0 earthquake, using the code PSGRN/PSCMP [*Wang et al.*, 2006].

For postseismic stress transfer simulation, we adopted linear Maxwell rheology to calculate the viscoelastic effects in this study. Although some other rheological models were suggested better to analyze postseismic relaxation processes, however, viscoelastic relaxation in timescale ~100 years shows minor differences in stress changes [*Verdecchia and Carena*, 2015]. Therefore, instead of following complex models incorporating additional unknowns, we go for simplest and primarily in practice linear Maxwell rheology. We assumed a viscosity of 1×10^{20} Pa · s for lower crust (η_{LC}) and upper mantle (η_M) because of lack of good constrains from geodetic observations. Different possible viscosities were tried for robustness of results.

3.2. Multilayered Lithospheric Model

Based on the Crust1.0, we built the lithospheric reference model that includes upper, middle, and lower crust and lithospheric mantle with the properties of density ρ, V_P, and V_s for each layer (Figure S1 in the supporting infromation). The lithospheric structure of location (96°E, 22°N), which is the central of the SF and Myanmar region, was adopted. The following expression is used to derive shear modulus (μ) by applying quantities: density (ρ) and V_P [*Aki and Richards*, 2002].

$$\mu = \rho Vs^2 \approx 1/3\ \rho Vp^2$$

We chose a Poisson's ratio of 0.25 and set a moderate value, 0.4, for effective coefficient of friction μ' [*King et al.*, 1994]. Furthermore, we inspect robustness of results by varying μ'.

4. Numerical Results

4.1. ΔCFS Evolution on SF

We calculated the stress transfer and accumulative ΔCFS using the parameters described above and shown in Table 1.

The ΔCFS evolution since the inception of earthquake series till 2003 earthquake on the SF is illustrated in Figure 2. A series of snapshots exhibit state of stress field by the initial event, 1906 M_w7.0, in Figure 2a followed by stress field state (Figures 2a–2i) immediately before each subsequent event. The 1906 earthquake ruptured the northern extreme of SF and significantly stressed the rupture of 1908 M_w7.5 earthquake. The coseismic ΔCFS associated with the 1906 and 1908 earthquakes posed impact mainly on the northern part of the SF (Figure 2b). Since the May 1930 earthquake located far from the ruptures of two previous earthquakes, our results show a negligible ΔCFS (~10^{-5} MPa) on the rupture of the May 1930 earthquake. Therefore, we suggested that the May 1930 earthquake is an independent one, which was not influenced by the two previous events in the sequence.

The May 1930 M_s7.4 earthquake, which ruptured the southern SF, loaded the whole rupture surface of the December 1930 M_s7.5 earthquake with coseismic ΔCFS over 0.01 MPa (Figure 2c). Since the time interval between these two events is only half year, the process of viscoelastic relaxation can be neglected. An average and maximum stress was raised up to 0.018 MPa and 0.066 MPa, respectively, due to coseismic loading on rupture surface (Table 1), going beyond 0.01 MPa (0.1 bar) above which earthquake triggering becomes statistically significant [*King et al.*, 1994; *Stein*, 1999; *Heidbach and Ben-Avraham*, 2007]. Consequently, the December 1930 M_s7.5 earthquake was evidently encouraged by the associated ΔCFS of the May 1930 M_s7.4 event.

The rupture of 1931 earthquake was stressed by the 1908 event, especially on its northern part. The 1931 earthquake significantly increased the stress accumulation north and southwest to its rupture plane (Figure 2e). The 1946 M_b7.5 earthquake occurred directly adjacent to the 1931 event. The coseismic ΔCFS increment on the rupture surface of 1946 M_b7.5 event is 0.018 MPa on average and 0.047 MPa in maximum. The process of postseismic viscoelastic relaxation further raised the ΔCFS by 19% immediately before the 1946 M_b7.5 event. The occurrence of 1946 M_b7.5 event made the lobe with increased ΔCFS migrate southward (Figure 2g). Another M_s7.8 earthquake occurred in this lobe immediately after the 1946 M_b7.5 event. The maximum ΔCFS increment on the rupture surface of 1946 M_s7.8 earthquake is larger than 0.25 MPa. It

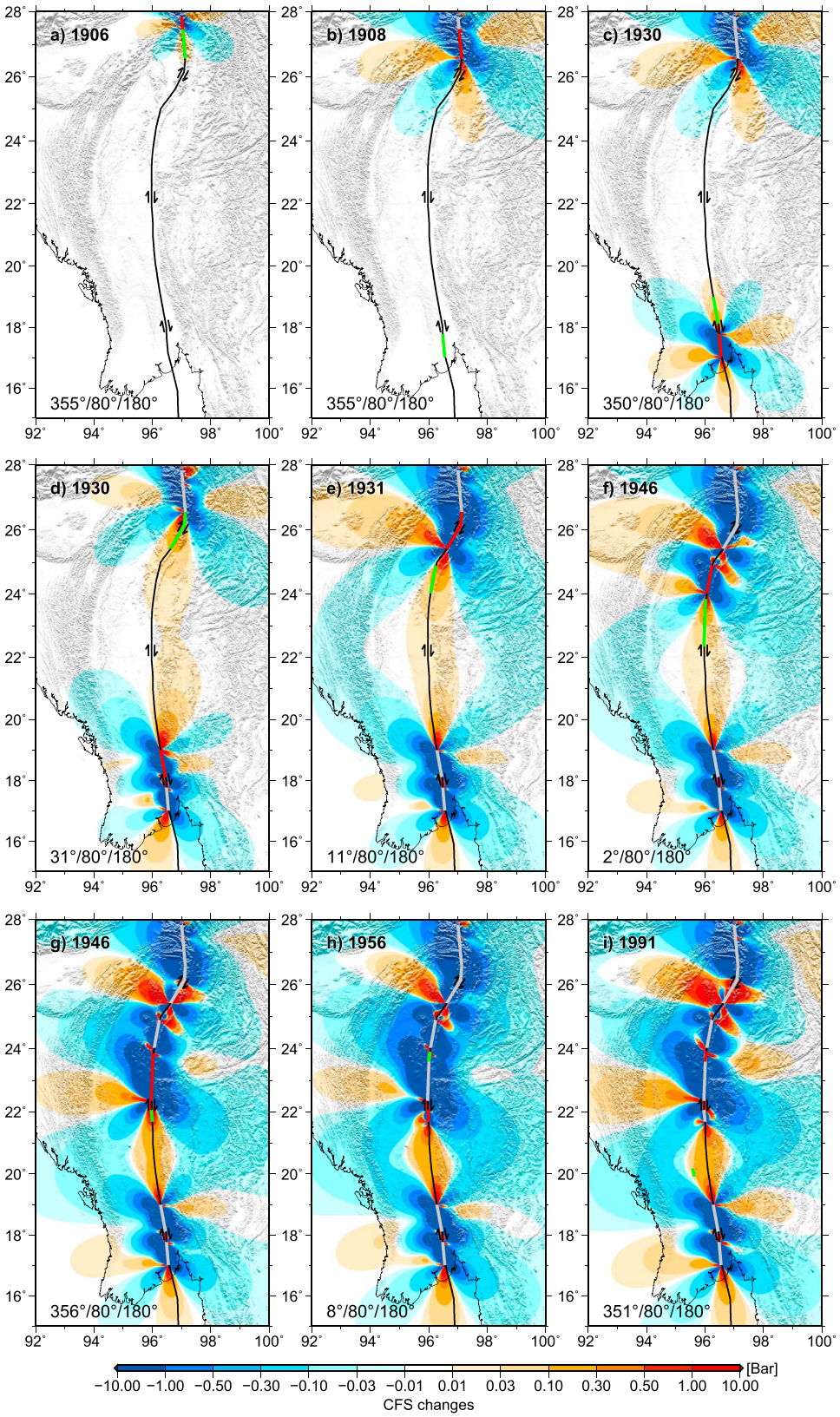

Figure 2. (a–i) ΔCFS evolution since 1906. The black thick line indicates the SF. The thick green, red, and gray lines represent the portion of the next earthquake rupture, the current earthquake rupture, and the previous ruptured portions, respectively. Figures 2a–2i indicate the ΔCFS immediately before the earthquake labeled by green thick lines; the label of year in each figure indicates the occurrence time of event labeled by red thick line.

means that the 1946 M_s7.8 earthquake was significantly encouraged by the 1946 M_b7.5 event. The 1946 M_s7.8 earthquake increased the ΔCFS accumulations to its south end, where an M_s7.0 earthquake occurred 10 years later. The coseismic ΔCFS increment on the rupture surface of 1956 M_s7.0 earthquake is up to 0.134 MPa on average and 0.283 MPa in maximum. The 1991 earthquake ruptured the small gap between the ruptures of two earthquakes in 1946. Although the rupture surface of 1991 earthquake is poorly constrained with some area overlapping the previous events, about 20% rupture surface of 1991 earthquake was still loaded by positive ΔCFS larger than 0.01 MPa. So we suggested that the 1991 earthquake may also encouraged by the previous events (Figure 2h). The ΔCFS transfer caused by the earthquakes from 1930 to 1991 stressed the rupture of the 2003 M_s6.8 earthquake. The coseismic ΔCFS increment on its rupture is 0.002 MPa in maximum. The process of postseismic stress transfer further raised the stress accumulation. Although the whole rupture of 2003 earthquake located in the regions with positive ΔCFS, both the maximum and average CFS increments are only 0.008 MPa. However, the high value of viscosity (1×10^{20} Pa · s) are adopted for both lower crust (η_{LC}) and upper mantle (η_M); this conservative assumption might induce the underestimation of contribution from postseismic viscoelastic relaxation. If lower viscosities are adopted, this earthquake might also be prompted by the preceding earthquakes (see the supporting information for detail).

In order to verify the applicability of earthquake triggering hypothesis to the SF, we combined both coseismic and postseismic ΔCFS in the investigation. We further categorized earthquake triggering based on the ΔCFS on rupture surface by following *Heidbach and Ben-Avraham* [2007]. We deduced that six out of nine events depict potential triggering owing to both average and maximum ΔCFS values greater than 0.01 MPa (Table 1). However, if we apply this scheme for the maximum ΔCFS changes on the rupture, eight out of nine events are potential examples of the earthquake triggering. It suggests that the preceding earthquakes prompt the occurrence of the following ones.

4.2. ΔCFS Accumulation and Seismic Hazard on SF

We extended the calculation to year of 2016 to further look into the ΔCFS accumulation on the SF (Figure 3a). Significant aspect of the cumulated ΔCFS on the fault is the existence of three positive ΔCFS sections, A–C (Figure 3). Sections A and C correspond to Meiktila Segment and Bago Segment, respectively. Section B manifest a doubtful pattern of the calculated ΔCFS pattern because the rupture extents of the two events in 1930 were not well constrained. Paucity of paleo-seismology and microseismicity information bounds us to conduct further quantitative investigation. Therefore, the state of ΔCFS and hazard of the section B still remains an open debatable question. However, the Meiktila Segment and Bago Segment are our interested regions which have faced the absence of any massive earthquake throughout the duration of 113 years [*Hurukawa and Maung Maung*, 2011].

The Meiktila Segment exists between 19.2°N and 21.5°N in central Myanmar. *Hurukawa and Maung Maung* [2011] outlined this region as a seismic gap with ~260 km long, corresponding to an *M*7.9 earthquake. Since Nay Pyi Taw, the new capital of Myanmar, and the highly populated city, Mandalay, locate near the Meiktila Segment, meaning that their populations are exposed to a significant earthquake hazard. Based on a paleo-seismological study, *Hurukawa and Maung Maung* [2011] proposed a recurrence interval of 160 years or more for this section. Since this region has not experienced any large earthquake over the past 113 years, the next large earthquake is expected to strike the area in the near future [*Hurukawa and Maung Maung*, 2011]. The earthquake-induced ΔCFS transfer would further increase the seismic hazard of this region. To quantify the influence from earthquake stress interaction, we model the rate of interseismic tectonic stress accumulation, and then compare it with earthquake-induced ΔCFS.

The tectonic stress loading was modeled by the deep dislocation technique proposed by *Savage* [1983] and was realized by a steady slip from the locking depth to 100 km. The slip increases from zero at the locking depth to its full magnitude at the bottom of crust [*Lorenzo-Martín et al.*, 2006]. In our simulation, the locking depth was set to be 15.5 km (bottom of upper crust), which is corresponding with the result from a GPS study in the central Myanmar [*Vigny et al.*, 2003]. Moreover, the focal depths of earthquakes occurred in this region are almost shallower than 15 km (http://www.globalcmt.org/CMTsearch.html). Therefore, the locking depth adopted in our model is relative reliable. The magnitude of the slip rates on the northern, central, and southern SF are set to be 16 mm/yr, 20 mm/yr, and 14 mm/yr, respectively [*Maurin et al.*, 2010]. The reference depth of tectonic loading simulation is set to be 10 km.

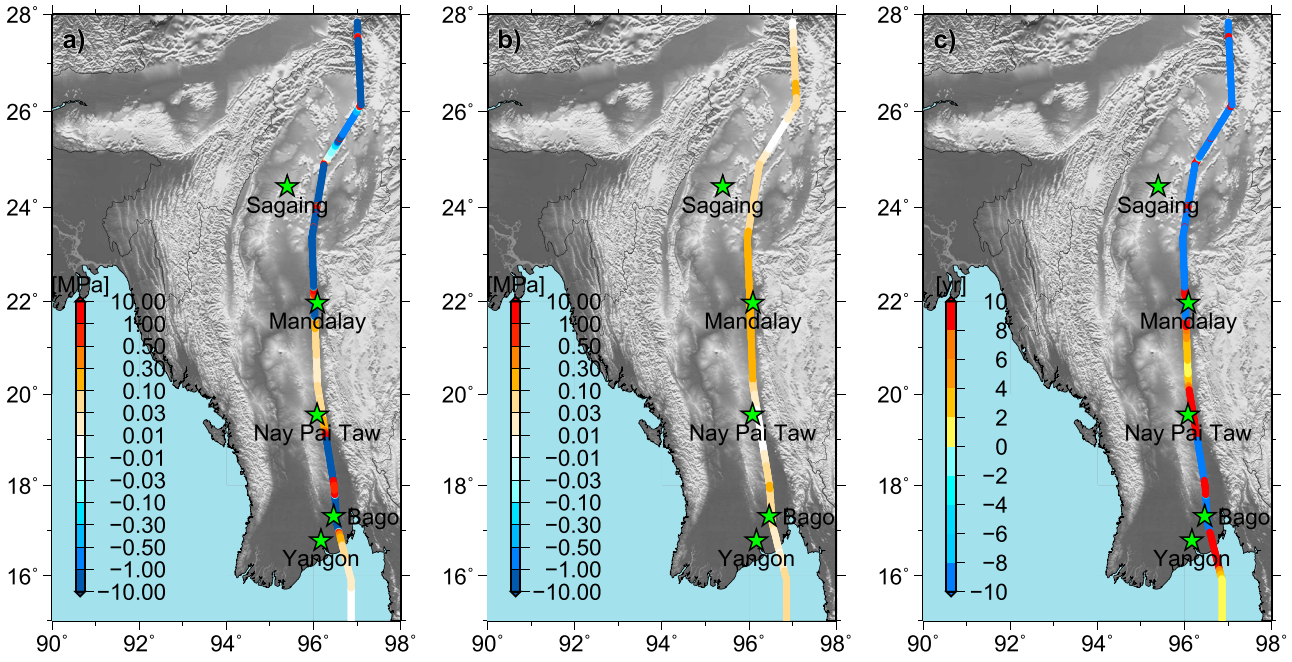

Figure 3. (a) ΔCFS (coseismic and postseismic) on the SF in the year of 2016. Units A–C are the three sections on which ΔCFS is significantly positive. (b) Stress accumulation on the SF caused by the tectonic loading of 10 years. (c) Time for tectonic loading being equivalent to the ΔCFS in Figure 3a. In this study, time for tectonic loading is calculated by dividing the earthquake-induced ΔCFS with the tectonic loading rate.

As shown in Figure 3c, the earthquake-induced ΔCFS prompts the Meiktila Segment and Bago Segment early to rupture. The encouragements for the northern and southern parts of the Meiktila Segment are more than 10 years. As mentioned above, this segment is on its later stage of earthquake cycle. The earthquake-induced ΔCFS could further enhance the probability of earthquake occurrence. The population of two neighboring cities, Mandalay and Nay Pyi Taw, is exposed to a severe earthquake hazard.

The Bago Segment is quite closed to Yangon (5.21 million populations) and Bago (1.225 million populations), the biggest and highest populated region in Myanmar. Considering the rupture of the whole segment range (~180 km), an earthquake of ~*M*7.7 is expected. The earthquake-induced ΔCFS obviously stressed the northern part of the Bago Segment, being equivalent to a tectonic loading over 10 years. Therefore, the northern extremity of the Bago Segment may be at risk to experience seismic hazard in near future.

4.3. Stability of the Results

The numerical results are prone to be affected by many factors. We conducted test experiments to examine the influence of two dominating factors, the coefficient of friction and the viscosities of lower crust and mantle, to verify the stability of the results.

4.3.1. Coefficient of Friction

Selection of suitable value for coefficient of friction μ' is significantly important for modeling results because it alters normal stress contribution to ΔCFS. Initially, we chose a commonly used value of 0.4 [*Parsons et al.*, 1999] for stress modeling and then conducted a series of investigation using values (0.2 and 0.6) to verify the robustness of outcomes. Numerical results reveal the difference ($<$10%) in calculated stress fields (Table 1). Therefore, impact of varying μ' is relatively small than other parameters such as slip distribution and rheology, hence, can be neglected.

4.3.2. Effect of Viscosity

The speed of the viscoelastic relaxation is mainly controlled by the viscosity of the lower crust and upper mantle: the smaller the viscosity, the quicker the relaxation process. Therefore, the choice of viscosity values may influence the results and needs to be justified. We tested our results by adopting various viscosity configurations (Table S1 in the supporting information). Our tests show that although the magnitude of ΔCFS changes, the choice of different viscosities does not influence the ΔCFS pattern and the triggering

relationship among our sequence for the timescale of the present study (~100 years), which is also verified by *Verdecchia and Carena* [2015] in their study of the California-Nevada border. Moreover, lower values of viscosities speed the relaxation process, leading to a more significant role of the postseismic viscoelastic relaxation for the buildup of ΔCFS (Table S1). However, for seismic hazard assessment, we prefer to deduce our results by using the higher value of viscosity (10^{20}Pa · s) for a conservative estimation.

5. Discussion and Conclusions

We further analyzed the ΔCFS imposed by some large neighboring historical earthquakes on the SF (black stars in Figure 1), including the 1762 M_w8.5 Arakan earthquake [*Wang*, 2013], 1897 *M*8.7 Assam earthquake [*Rajendran et al.*, 2004], 1950 *M*8.6 Assam–Tibet earthquake [*Raghukanth*, 2008], 1912 M_w7.7 Burma [*Wang*, 2013], 2004 M_w9.2 Aceh, and 2005 M_w8.7 Nias earthquakes on the Sumatra-Andaman-Sagaing fault system [*Cattin et al.*, 2009].

Despite great magnitudes, the 2004 Aceh and 2005 Nias earthquakes only stressed the southernmost part of the SF, but the magnitude is negligible [*Cattin et al.*, 2009]. The 1762 M_w8.5 earthquake slightly raised ΔCFS on the central part of SF (~0.003 MPa). The influence from 1897 M8.7 earthquake on SF is also negligible ($<1 \times 10^{-4}$ MPa). The 1912 M_w7.7 earthquake stressed the southern part of the Meiktila Segment by 0.01 MPa but reduced the ΔCFS accumulation on its northern part with 0.03 MPa. The 1950 *M*8.6 earthquake obviously reduced the CFS accumulation on northern extreme of SF (>0.2 MPa).

We also investigated the influence of the potential large earthquake on the Sunda Trench upon the ΔCFS on the SF. *Steckler et al.* [2016] proposed an underappreciated hazard existed between Indian Plate and Myanmar. An earthquake with $M_w > 8.2$ may occur on the locked megathrust below the fold belt (red dashed line in Figure 1). We calculated the ΔCFS on the SF caused by the potential earthquake on the Sunda Trench and found that the earthquake would reduce the ΔCFS accumulation (≤0.01 MPa) on the southern part of the Bago Segment and slightly stress its northern part (~10^{-3} MPa). It means that the potential earthquake on Sunda Trench has little influence on the SF in the future.

Thus, we can conclude that the neighboring large earthquakes do not significantly affect the ΔCFS on the SF, confirming the robustness of our results.

In summary, we calculated the coseismic and postseismic ΔCFS evolution in the SF area to test the stress triggering hypothesis by using a sequence of 10 historical earthquakes along the SF from 1906 to 2003. The earthquake interaction analysis reveals that eight out of nine earthquakes posterior to the 1906 earthquake show encourage effects owing to the maximum cumulative ΔCFS on the rupture. A good correlation between ΔCFS transfer and earthquake occurrence and a significant interaction between earthquakes are demonstrated.

From the cumulative ΔCFS on the SF, we unveiled three sections with notable ΔCFS increment in central and southern SF. Since these highly populated regions have not experienced any large earthquake throughout period of 113 years, and the earthquake-induced ΔCFS further raised the stress accumulation on these segments, the seismic hazard in these areas is emphasized.

Acknowledgments
We thank the Editor Andrew V. Newman and two anonymous reviewers for their insightful review and thoughtful comments that helped us greatly to improve the focus and quality of the manuscript. This work is supported by the National Natural Science Foundation of China (grants 41274104, 41541034, and 41574095). Figures were plotted with the Generic Mapping Tools [*Wessel and Smith*, 1998].

References

Aki, K., and P. G. Richards (2002), *Quantitative Seismology Second Edition*, 73 pp., Univ. Science Books, Sausalito, Calif.

Cattin, R., N. Chamot-Rooke, M. Publier, A. Rabaute, M. Delescluse, C. Vigny, L. Fleitout, and P. Dubernet (2009), Stress change and effective friction coefficient along the Sumatra-Andaman-Sagaing fault system after the 26 December 2004 (M_w = 9.2) and the 28 March 2005 (M_w = 8.7) earthquakes, *Geochem. Geophys. Geosyst.*, *10*, Q03011, doi:10.1029/2008GC002167.

Curray, J. R. (2005), Tectonics and history of the Andaman Sea region, *J. Asian Earth Sci.*, *25*(1), 187–232.

Deng, J., and L. R. Sykes (1996), Triggering of 1812 Santa Barbara earthquake by a great San Andreas shock: Implications for future seismic hazards in southern California, *Geophys. Res. Lett.*, *23*, 1155–1158, doi:10.1029/96GL00738.

Freed, A. M. (2005), Earthquake triggering by static, dynamic and postseismic stress transfer, *Annu. Rev. Earth Planet. Sci.*, *33*, 335–367.

Harris, R. A., R. W. Simpson, and P. A. Reasenberg (1995), Influence of static stress changes on earthquake locations in southern California, *Nature*, *375*, 221–224.

Heidbach, O., and A. Ben-Avraham (2007), Stress evolution and seismic hazard of the Dead Sea fault system, *Earth Planet. Sci. Lett.*, *257*, 299–312.

Holt, W. E., F. N. James, T. C. Wallace, and A. J. Haines (1991), The active tectonics of the eastern Himalayan syntaxis and surrounding regions, *J. Geophys. Res.*, *96*(B9), 14,595–14,632, doi:10.1029/91JB01021.

Hurukawa, N., and P. Maung Maung (2011), Two seismic gaps on the Sagaing Fault, Myanmar, derived from relocation of historical earthquakes since 1918, *Geophys. Res. Lett.*, *38*, L01310, doi:10.1029/2010GL046099.

Kanamori, H., and D. L. Anderson (1975), Theoretical basis of some empirical relations in seismology, *Bull. Seismol. Soc. Am.*, *65*, 1073–1095.
King, G. C. P., R. S. Stein, and J. Lin (1994), Static stress changes and the triggering of earthquakes, *Bull. Seismol. Soc. Am.*, *84*, 935–953.
Kundu, B., and V. K. Gahalaut (2012), Earthquake occurrence processes in the Indo-Burmese wedge and Sagaing fault region, *Tectonophysics*, *524–525*, 135–146.
Lorenzo-Martín, F., F. Roth, and R. J. Wang (2006), Elastic and inelastic triggering of earthquakes in the north Anatolian fault zone, *Tectonophysics*, *424*, 271–289.
Maung, H. (1987), Transcurrent movements in the Burma-Andaman Sea region, *Geology*, *15*(10), 911–912.
Maurin, M., F. Masson, C. Rangin, U. T. Min, and P. Collard (2010), First global positioning system results in northern Myanmar: Constant and localized slip rate along the Sagaing fault, *Geology*, *38*(7), 591–594.
Mitchell, A. H. G. (1993), Cretaceous-Cenozoic tectonic events in the western Myanmar (Burma)-Assam region, *J. Geol. Soc.*, *150*, 1089–1102.
Nalbant, S. S., S. Steacy, J. McCloskey, K. Sieh, and D. Natawidjaja (2005), Earthquake risk on the Sunda trench, *Nature*, *435*(7043), 756–757.
Parsons, T., R. S. Stein, R. W. Simpson, and P. A. Reasenberg (1999), Stress sensitivity of fault seismicity: A comparison between limited-offset oblique and major strike-slip faults, *J. Geophys. Res.*, *104*(20), 183–202.
Pollitz, F., M. Vergnolle, and E. Calais (2003), Fault interaction and stress triggering of twentieth century earthquakes in Mongolia, *J. Geophys. Res.*, *108* (B10), 2503, doi:10.1029/2002JB002375.
Raghukanth, S. T. G. (2008), Simulation of strong ground motion during the 1950 great Assam earthquake, *Pure Appl. Geophys.*, *165*, 1761–1787.
Rajendran, C. P., K. Rajendran, B. P. Duarah, S. Baruah, and A. Earnest (2004), Interpreting the style of faulting and paleoseismicity associated with the 1897 Shillong, northeast India, earthquake: Implications for regional tectonism, *Tectonics*, *23*, TC4009, doi:10.1029/2003TC001605.
Savage, J. C. (1983), A dislocation model of strain accumulation and release at a subduction zone, *J. Geophys. Res.*, *88*, 4984–4996.
Scholz, C. H. (1990) *The Mechanics of Earthquakes and Faulting*, 439 pp., Cambridge Univ. Press, New York.
Searle, M. P., S. R. Noble, J. M. Cottle, D. J. Waters, A. H. G. Mitchell, T. Hlaing, and M. S. A. Horstwood (2007), Tectonic evolution of the Mogok metamorphic belt, Burma (Myanmar) constrained by U-Th-Pb dating of metamorphic and magmatic rocks, *Tectonics*, *26*, TC3014, doi:10.1029/2006TC002083.
Shan, B., X. Xiong, R. J. Wang, Y. Zheng, and S. Yang (2013), Coulomb stress evolution along Xianshuihe–Xiaojiang fault system since 1713 and its interaction with Wenchuan earthquake, May 12, 2008, *Earth Planet. Sci. Lett.*, *377–378*(5), 199–210.
Steckler, M. S., D. R. Mondal, S. H. Akhter, L. Seeber, L. J. Feng, J. Gale, E. M. Hill, and M. Howe (2016), Locked and loading megathrust linked to active subduction beneath the Indo-Burman ranges, *Nat. Geosci.*, doi:10.1038/ngeo2760.
Stein, R. S. (1999), The role of stress transfer in earthquake occurrence, *Nature*, *402*, 605–609.
Stein, R. S. (2003), Earthquake conversations, *Sci. Am.*, *288*, 72–79.
Tsutsumi, H., and T. Sato (2009), Tectonic geomorphology of the southernmost Sagaing fault and surface rupture associated with the May 1930 Pegu (Bago) earthquake, Myanmar, *Bull. Seismol. Soc. Am.*, *99*, 2155–2168, doi:10.1785/0120080113.
Toda, S., R. S. Stein, P. A. Reasonberg, and J. H. Dieterich (1998), Stress transferred by the M_w = 6.5 Kobe, Japan, shock: Effect on aftershocks and future earthquake probabilities, *J. Geophys. Res.*, *103*, 24,543–24,565.
Verdecchia, A., and S. Carena (2015), One hundred and fifty years of Coulomb stress history along the California-Nevada border, USA, *Tectonics*, *34*, 213–231, doi:10.1002/2014TC003746.
Vigny, C., A. Socquet, C. Rangin, N. Chamot-Rooke, M. Pubelier, M. N. Bouin, G. Bertrand, and M. Becker (2003), Present day crustal deformation around Sagaing fault, Burma, *J. Geophys. Res.*, *108*(B11), 2533, doi:10.1029/2002JB001999.
Wang, R., F. Lorenzo-Martín, and F. Roth (2006), PSGRN/PSCMP—A new code for calculating co- and post-seismic deformation, geoid and gravity changes based on the viscoelastic-gravitational dislocation theory, *Comput. Geosci.*, *32*, 527–541.
Wang, Y. (2013), Earthquake geology of Myanmar, PhD dissertation, California Institute of Technology.
Wells, D. L., and K. J. Coppersmith (1994), New empirical relationships among magnitude, rupture length, rupture width, rupture area, and surface displacement, *Bull. Seismol. Soc. Am.*, *84*, 974–1002.
Wessel, P., and W. H. F. Smith (1998), New improved version of Generic Mapping Tools released, *Eos. Trans. AGU*, *79*, 579, doi:10.1029/98EO00426.